http://doi.org/10.35784/iapgos.7612 *received: 22.04.2025 | revised: 19.01.2026 | accepted: 16.04.2026 | available online: 30.06.2026*

PERFORMANCE EVALUATION OF OPTIMIZED DEEP LEARNING MODEL WITH MULTILAYERED MAX-NORM REGULARIZATION (MMNR) TECHNIQUE FOR BRAIN TUMOUR CLASSIFICATION IN MRI MULTI-MODAL IMAGES

Mulackal Chandran Binish[1], Vinu Thomas[2]
[1]APJ Abdul Kalam Technological University, Model Engineering College, Kerala, India, [2]APJ Abdul Kalam Technological University, Kerala, India

Abstract. *Brain tumours are aggressive malignant diseases, both in children and adults, representing 86 to 92 percent of all primary and almost half of secondary Central Nervous System (CNS) tumours. For individuals with malignant brain or central nervous system (CNS) tumours, the 5-year survival rate is about 34% for males and 36% for women. Brain tumours can be classified into several types, including benign, malignant, pituitary, etc. This study proposes a new architecture named Multilayered Max-Norm Regularization CNN (MMNR-CNN) and investigates the performance of this model for the classification of brain tumours in multi-modal MRI images. The model incorporates Markov Random Field (MRF) for bias field correction, and Monte Carlo Dropout to quantify prediction uncertainty through stochastic forward passes, enhancing the model's reliability in clinical decision-making. Furthermore, we integrate Explainable AI (XAI) techniques using Gradient-weighted Class Activation Mapping (Grad-CAM) to visually interpret the regions of MRI scans that contribute most to the classification decisions. We present a complete analysis of the Multilayered Max-Norm Regularization model trained on augmented brain image data and compare the performance on different values of regularization parameters that lead to the automatic selection of spatially important features for the classification task. This increases the generalization and robustness of the training dataset through augmentation. The model is trained using the Br35H database and the Figshare database. Both are used primarily for research in brain tumour detection and classification. The obtained performance metrics are the best in the literature, with a testing accuracy of 99.88% and 100 % precision.*

Keywords: MRI images, deep learning, fine-tuned model training, data augmentation, regularization

OCENA WYDAJNOŚCI ZOPTYMALIZOWANEGO MODELU GŁĘBOKIEGO UCZENIA SIĘ Z WIELOWARSTWOWĄ TECHNIKĄ OGRANICZENIA NORMY MAKSYMALNEJ (MMNR) DO KLASYFIKACJI GUZA MÓZGU W OBRAZACH WIELOMODALNYCH MRI

Streszczenie. *Guzy mózgu to agresywne choroby złośliwe, zarówno u dzieci, jak i u dorosłych, stanowiące 86–92% wszystkich pierwotnych i prawie połowę wtórnych guzów ośrodkowego układu nerwowego (OUN). U osób ze złośliwymi guzami mózgu lub ośrodkowego układu nerwowego (OUN) 5-letni wskaźnik przeżycia wynosi około 34% dla mężczyzn i 36% dla kobiet. Guzy mózgu można podzielić na kilka typów, w tym łagodne, złośliwe, przysadkowe itp. W niniejszym badaniu zaproponowano nową architekturę o nazwie Wielowarstwową Techniką Ograniczenia Normy Maksymalnej (Multilayered Max-Norm Regularization CNN – MMNR-CNN) i zbadano wydajność tego modelu w klasyfikacji guzów mózgu w wielomodalnych obrazach MRI. Model wykorzystuje losowe pole Markowa (MRF) do korekcji pola błędu oraz metodę Monte Carlo Dropout do ilościowego określania niepewności prognozy poprzez stochastyczne przejścia do przodu, zwiększając niezawodność modelu w podejmowaniu decyzji klinicznych. Ponadto integrujemy techniki XAI (Exploreable AI) wykorzystujące Gradient-weighted Class Activation Mapping (Grad-CAM), aby wizualnie zinterpretować obszary skanów MRI, które mają największy wpływ na decyzje klasyfikacyjne. Przedstawiamy pełną analizę modelu MMNR wytrenowanego na rozszerzonych danych obrazowych mózgu i porównujemy wydajność przy różnych wartościach parametrów regularyzacji, które prowadzą do automatycznego wyboru cech istotnych przestrzennie dla zadania klasyfikacji. Zwiększa to generalizację i odporność zbioru danych treningowych poprzez rozbudowę. Model jest trenowany z wykorzystaniem bazy danych Br35H i Figshare. Obie są wykorzystywane głównie w badaniach nad wykrywaniem i klasyfikacją guzów mózgu. Uzyskane wskaźniki wydajności są najlepsze w literaturze, z dokładnością testowania na poziomie 99,88% i 100% precyzją.*

Słowa kluczowe: obrazy MRI, głębokie uczenie, trening precyzyjnie dostrojonych modeli, rozszerzanie danych, regularyzacja

Introduction

The most important clinical application for diagnosing, treating, and managing patients with brain tumours is the classification of their MRI images. Appropriate classification of brain tumours will not only lead to correctness in determining treatment but also make it possible to reduce the mortality rate and effectively improve the clinical treatment outcome [23]. Deep learning techniques have shown great success in medical image analysis, including the classification of brain tumours [22]. Magnetic Resonance Imaging (MRI) is widely regarded as the gold standard for brain tumour detection due to its superior ability to differentiate between various soft tissues in the brain [19, 21]. MRI scans provide detailed images across multiple modalities, such as T1-weighted, T2-weighted, and FLAIR (Fluid-Attenuated Inversion Recovery) images, each offering unique information critical for accurate diagnosis [20]. However, the manual examination of these images by radiologists can be both time-consuming and prone to error, given the intricate nature of brain structures and the subtle variations between healthy and tumorous tissues [2].

The accuracy and productivity of medical image analysis have shown considerable promise for automated classification systems that make use of machine learning (ML) and artificial intelligence (AI). These developments have been led by Deep Learning (DL), in particular by its capacity to extract intricate patterns from massive datasets. Brain tumour classification is one of the many medical imaging tasks that Convolutional Neural Networks (CNNs), a kind of deep learning model created especially for image processing, have repeatedly shown superior performance in [17].

This study proposes a Multilayered Max-Norm Regularization for balanced bias and variance with a layer-by-layer analysis approach to classify brain tumours using multimodal MRI images from the Br35H database, available on Kaggle. Our architecture is augmented to handle the complexities of multimodal MRI data, incorporating techniques such as data augmentation and fine-tuning using L2 regularization on each layer of the model with variable regularization parameters. The BR35H dataset is a comprehensive collection of MRI scans that includes various brain tumour images, categorized into two classes: tumour-present and tumour-absent.

Regularization is essential in deep learning to prevent overfitting and improve the generalization capabilities of models. Regularization methods penalize the model complexity, ensuring it doesn't fit the training data too closely. By preventing overfitting, regularization enhances the model's ability to generalize well to new, unseen data and also stabilizes the training process, especially when dealing with noisy or limited data.

In order to solve this uncertainty in medical predictions, we use Monte Carlo (MC) Dropout in our model so that we can have stochastic forward passes during inference. Besides the accuracy of performance, another issue when it comes to AI-assisted diagnostics is interpretability. In this respect, our architecture

incorporates the methods of Explainable AI (XAI) with Gradient-weighted Class Activation Mapping (Grad-CAM).

This Monte Carlo provides a principled estimation of predictive uncertainty, which is vital in real-world clinical decision-making. By quantifying the model's confidence in each prediction, clinicians can better interpret the reliability of automated outputs and prioritize ambiguous cases for further review. The XAI approach highlights the spatial regions of MRI scans that most strongly influence the model's decisions [20], offering visual explanations that align with clinical intuition and increasing trust in the model's outputs.

Figure 1 shows various brain tumour images from the Br35H dataset, highlighting the diversity in tumour appearance and structure. The tumour regions are visible as intensity enhanced within the concentrated locations. This poses significant challenges to the design of a robust classification model due to the heterogeneity of tumours, involving significant variability in size, shape, location, and appearance. Various MRI sequences reflect brain anatomy and pathology differently; hence, accurate classification must be done based on their combined evaluation. In addition, some types of tumours have overlapped characteristics with others, so they cannot be discriminated only by imaging. Variability in image quality due to patient movement or differences in the imaging equipment will only serve to occlude the critical features necessary for classification.

Another level of complexity is due to intratumoural heterogeneity, where different regions within a single tumour can have different characteristics. This is necessitated by the intricate anatomy of the brain, the imbalances in class datasets, and the presence of some tumours that might have very subtle differences. Then, it brings further issues of ensuring clinical relevance for actionable insights from classification results that require advanced techniques and interdisciplinary collaboration. Our augmented and multilayered Max-Norm Regularization CNN(MMNR-CNN) model achieved an impressive testing accuracy score of 99.88%, indicating its potential effectiveness in clinical settings. The performance of our model is measured by key metrics, namely: accuracy, sensitivity, recall, and specificity. Our results show that significant improvements in classification performance can be achieved as the data augmentation and layer-by-layer diverse regularization technique included in brain tumour classification tasks are proven effective.

The rest of the article is organized as follows: In Section 2, relevant research in the field of CNN-based data augmentation and brain tumour classification is reviewed. Section 3 details the methodology, including data preprocessing, the CNN architecture, and the augmentation techniques applied. The experimental findings and performance assessment are shown in Section 4. The results, difficulties, and future directions are covered in Section 5. Finally, section 6 concludes the study, summarizing the key contributions and implications of medical imaging and diagnostics.

1. Related works

The brain tumours can influence the quality and duration of life as they are formed when the cells in the area of the head grow excessively. The patients whose brain tumours are misdiagnosed or diagnosed late as well as patient who are not treated show less opportunity to survive. MR imaging equipment provides pictures which are usually used to detect brain cancers [9].

The model modification suggested by A. K. Sharma [26] addressed certain issues related to the brain tumour classification, i.e., class imbalance and the necessity to accurately differentiate between various types of tumours. Although the exact changes to the ResNet50 architecture have not been introduced in the paper, the consideration of the transfer learning indicates that the focus was put on the adaptability of the pre-trained models to the unique features of brain MRI data.

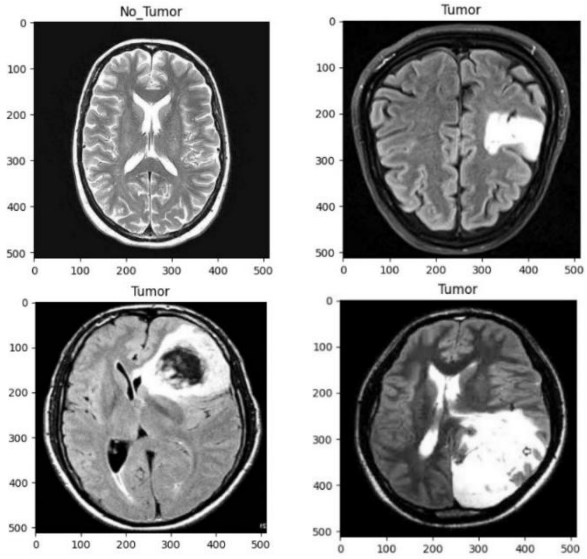

Fig. 1. MRI images with tumour and no tumour from Br35H database

Louis D. N. et al. [19] provided a comprehensive summary of the World Health Organization summit and detailed analysis and Classification of Tumours of the Central Nervous System. This classification serves as a fundamental reference for understanding brain tumour pathology and guides subsequent research and clinical practice. Menze B. H. et al. presented the Brain Tumour Segmentation competition (BRATS 2014) in their paper [21]. This benchmark dataset has been essential in helping to advance the area of medical image analysis by assessing and contrasting various brain tumour segmentation techniques. This paper shows how deep learning techniques may be used to increase tumour classification accuracy and efficiency, which is important for prognosis and treatment planning. Chang et al. [7] proposed a residual convolutional neural network for determining IDH status in gliomas using MR imaging. This work demonstrates the utility of deep learning techniques for predicting molecular markers associated with tumour behaviour, which has important implications for personalized treatment strategies.

An overview of deep convolutional neural networks for computer-aided detection was presented by Shin et al. [27], with particular attention to CNN designs, dataset characteristics, and transfer learning. Multimodal Deep learning models are also addressed in [31] for the classification of MRI of Alzheimer's disease. A hybrid model of GoogLeNet architecture is discussed in Amran G. A. et al. [4] with a CNN incorporated and obtained a classification accuracy 99.51%.

A review highlights the potential of deep learning models for improving diagnostic accuracy and efficiency in medical imaging applications is presented in [17]. A Caps net-based model SA-CapsGAN operated on MNIST data is presented in [28] and shows the performance of self-attention. Majority voting implementation on pre trained models for brain tumour classification is presented in [30]. CNN with transfer learning characteristics applications is discussed in [27]. Peritumoural MRI analysis is presented in [1] with images processing for recognizing surface irregularities.

For precise brain lesion segmentation, Kamnitsas et al. [15] suggested combining an effective multi-scale 3D CNN with a fully linked CRF. Analysis of common models for brain tumour detection are discussed in [24] and concluded DensNet121 as the best performing model with some modifications.

Precise lesion delineation in medical imagery is a difficulty that needs to be addressed in order to design treatments and track the evolution of diseases. Zhou et al. [33]. presented a stacked U-Net architecture for medical image segmentation called UNet++. This architecture improves upon the traditional U-Net model by incorporating nested skip pathways, leading to more accurate and robust segmentation results. Havaei et al. [13]

suggested brain tumour segmentation using deep neural networks and showed that deep learning approaches are effective for automated tumour segmentation in medical imagery.

Havaei et al. [14] introduced HeMIS, a hetero-modal image segmentation method, which extends traditional image segmentation techniques to handle multi-modal medical images for improved segmentation accuracy. Brain Tumour segmentation using Brats2018 database are implemented in [25] and dice score of all tumour classes are computed. GLCM based CNN models for brain tumour classification models are discussed in [5] and evaluated the Figshare and Br35H database.

Akbari et al. [1] conducted a study on pattern analysis of dynamic susceptibility of images in contrast-enhanced MRI images to demonstrate peritumoural tissue heterogeneity, providing insights into brain tumour microenvironments' complex spatial and temporal dynamics. Neural network approaches of brain tumour classification are discussed in [8] with relevance to explainable AI. Spatial and Temporal approaches of caps network is discussed in [10] and this network shows high results on 3 databases for action recognition.

3D capsule network for prostate detection gives high accuracy by implementing self-attention as presented in [16]. Zhang et al. [31] proposed a deep learning and ML-based multi-modal brain tumour classification method using MRI images, exploring the potential of deep learning and ML techniques for integrating information from different imaging modalities for improved tumour classification accuracy. Ghafoorian et al. [11] investigated transfer learning for domain adaptation in MRI, demonstrating its application in brain lesion segmentation and highlighting its potential for improving segmentation accuracy across different imaging domains.

Table 1. Comparison of brain tumour classification methods during 2019–2024

Paper (Year)	Method	Accuracy (%)	Precision (%)	Recall (%)
Sharif et al. (2020) [25]	Active Deep Neural Network	98.0	97.0	97.5
Shah et al. (2022) [23]	Fine-tuned EfficientNet	97.8	96.5	97.0
Tandel et al. (2021) [30]	Majority Voting, Deep Learning	96.1	94.5	95.5
Zhang et al. (2022) [32]	Single Model Deep Learning	92.8	91.2	91.8
Ammar et al. (2024) [3]	ViT Ensemble Model	98.7	97.8	98.3
Das et al. (2024) [8]	NASNet	99.6	98.9	99.3
Li et al. (2023) [16]	CapsNet with MRI	90.9	89.5	90.2
Sun et al. (2021) [28]	Modified CapsNet	91.8	90.4	91.0
Feng et al. (2023) [10]	Spatial & temporal CapsNet	78.0	76.5	77.2
Amran et al. (2022) [4]	Hybrid GoogLeNet architecture	99.51	99	98.90
Ata et al. (2023) [5]	GLCM-based CNN	98.22	97.11	98.91

2. Methodology

We used the Br35H database as described earlier, which is a publicly available dataset that provides a large collection of MRI images specifically aimed at facilitating research in the area of brain tumour detection, segmentation, and classification. It is designed to support machine learning and deep learning model development by providing high-quality, annotated imaging data. It consists of 3000 images of both benign and malignant, of which 1500 are with tumours and 1500 are without tumours. The data is split for training and testing. 70% of the data, which is 2100, is used for training, and 30% of the data, which is 900, is used for testing and validation.

Our data augmentation process involved various techniques to introduce variability into the training dataset, thereby enhancing the model's robustness. Initially, we performed Z-score normalization on training and test data sets. Geometric transformations such as rotations, translations, and scaling were applied to simulate different perspectives of the MRI images. This helps the model learn to recognize tumours from various angles and positions. The augmentation techniques included geometric transformations such as rotations (e.g., ±10 degrees), translations (e.g., ±10 pixels horizontally and vertically), and scaling (e.g., zoom in/out by 10–20%). The augmentation techniques included the following.

2.1. MRF and Z-score normalization

Magnetic resonance images (MRI) commonly exhibit low-frequency intensity inhomogeneity (bias field) that degrades segmentation and quantitative analysis. Probabilistic methods that jointly estimate tissue labels and the bias field are particularly effective among these. Markov Random Field (MRF) priors provide a natural way to impose spatial coherence on both tissue labels and the estimated field.

Let $(I(x))$ denote the observed intensity at the voxel (x), $(B(x))$ the multiplicative bias field, $(R(x))$ the true underlying (bias-free) tissue intensity, and $(L(x) \in \{1, \ldots, K\})$ the discrete tissue label (e.g., CSF, GM, WM). The observation model is

$$I(x) = B(x)\,R(x) + \varepsilon(x) \quad (1)$$

where $(\varepsilon(x))$ is additive noise (commonly modeled as Gaussian or, for magnitude MRI, Rician-approximated). We model tissue intensities with a class-conditional Gaussian:

$$p(R(x) \mid L(x) = k) = \mathcal{N}(\mu_k, \sigma_k^2) \quad (2)$$

Equivalently, after log-transforming to decouple multiplicative bias

$$\log I(x) \approx \log B(x) + \log R(x) + \eta(x) \quad (3)$$

Spatial priors are introduced via MRFs. For labels, a Potts-like prior encourages neighbouring voxels to share the same label:

$$P(L) \propto \exp\left(-\beta \sum_{\langle x,y \rangle} 1\{L(x) \neq L(y)\}\right) \quad (4)$$

where $(\langle x, y \rangle)$ denotes neighbouring voxels and $(\beta > 0)$ is the smoothing weight. For the bias field, a Gaussian Markov prior or quadratic smoothness prior is typical:

$$P(B) \propto \exp\left(-\lambda \sum_{\langle x,y \rangle} (B(x) - B(y) \backslash big)^2\right) \quad (5)$$

which enforces that $(B(x))$ varies slowly across space. The maximum a posteriori (MAP) objective becomes

$$(\hat{B}, \hat{L}) = \\ = \arg\max_{B,L} 1\,[\log p(I \mid B, L) + \log P(B) + \log P(L)] \quad (6)$$

A practical and widely-used inference strategy alternates between estimating label probabilities and updating the bias field, commonly realized as an EM-like scheme with MRF regularization:

E-step (Label estimation): Given the current bias estimate $(B^{(t)})$, compute posterior label probabilities using the likelihood $(p(I(x) \mid B^{(t)}, L(x) = k)$ and the MRF prior. Approximate inference methods include Iterated Conditional Modes (ICM), loopy belief propagation, or graph-cut-based optimization for the Potts model.

M-step (Bias update): Given soft label assignments (or hard labels) estimate the bias field $(B(x))$ by maximizing the expected log-likelihood with a smoothness penalty. In the log-domain, this is commonly a penalized least-squares problem and can be solved by B-spline fitting or by solving a linear system with regularization. Iterate until convergence (changes in labels/bias norm below threshold).

Z-score normalization, also known as standardization, is a common technique used in data preprocessing to rescale features so that they have the properties of a standard normal distribution with a mean of 0 and a standard deviation of 1. It standardizes the range of independent variables/features in the images, ensures that each feature contributes equally to the analysis, and avoids the dominance of features with larger scales or variances.

The Z-score normalization can be summarized as

$$\mathbf{z} = (\mathbf{x} - \mu)/\,\boldsymbol{\sigma} \quad (7)$$

Calculation of the mean μ of the dataset

$$\boldsymbol{\mu} = \frac{1}{N}\sum_{i=1}^{N} \boldsymbol{x_i} \quad (8)$$

Calculation of the standard deviation σ of the dataset

$$\boldsymbol{\sigma} = \sqrt{\frac{1}{N}\sum_{i=1}^{N}(x_i - \boldsymbol{\mu})^2} \quad (9)$$

Figures 2–5 demonstrate the transformation of brain MRI images through z-score normalization, which is a crucial preprocessing step in our work. Figure 2 and Figure 4 show the original images from the BR35H database. Figure 3 and Figure 5 display the corresponding z-score normalized images. This normalization enhances the contrast and clarity of the images, aiding in more accurate medical image analysis, and enhances the spatially distributed features.

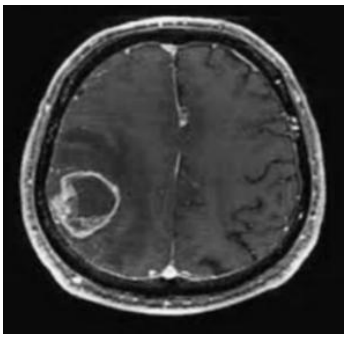

Fig. 2. Brain MR image without tumour

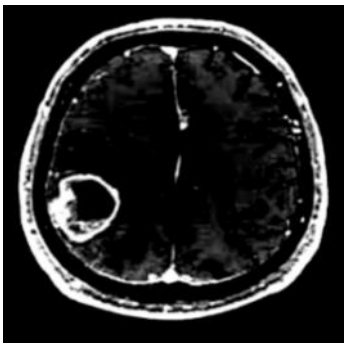

Fig. 3. Z-score normalized image showing the intensity variation

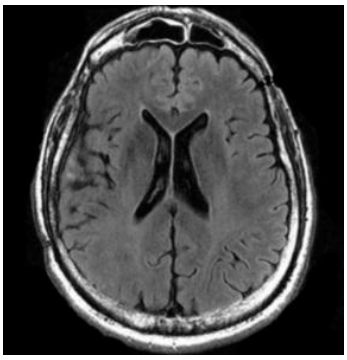

Fig. 4. Brain MR image with tumour

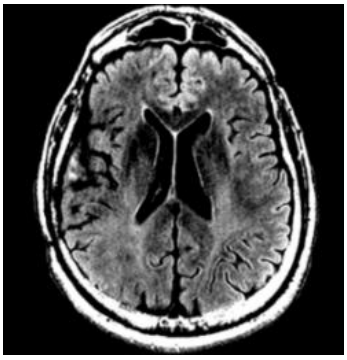

Fig. 5. Z-score normalized image showing the intensity variation

2.2. Geometric transformations

Geometric transformations such as Rotations, Translations, and Scaling were applied to the whole image database. Rotations were applied to simulate different orientations of the MRI images. The rotation of an image by an angle ϕ (in degrees) can be represented by the following transformation matrix.

$$R(\phi) = [\cos\phi \ -\sin\phi;\ sin\phi \ \ cos\phi] \quad (10)$$

Translations were applied to shift the image horizontally and vertically. The translation of an image by (tm, tn) pixels can be represented by the following transformation matrix:

$$T(tm, tn) = [1\ 0\ t\_m;\ 0\ 1\ t\_n;\ 0\ 0\ 1] \quad (11)$$

Scaling was applied to zoom in and out of the image. The scaling of an image by factors *Sx* and *Sy* can be represented by the following transformation matrix:

$$S(sx, sy) = [Sx \quad 0;\ 0 \ \ Sy] \quad (12)$$

These transformations simulate variations in image acquisition and help the model generalize better by exposing it to different perspectives of the same data, and the trans formed images are shown in Fig. 6 and 7. These augmentations were applied in real-time during training, introducing variability and preventing overfitting, thereby improving the model's performance and robustness.

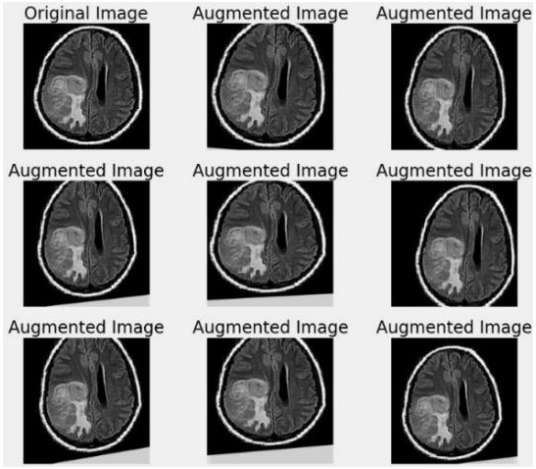

Fig. 6. Augmented images after translation and scaling

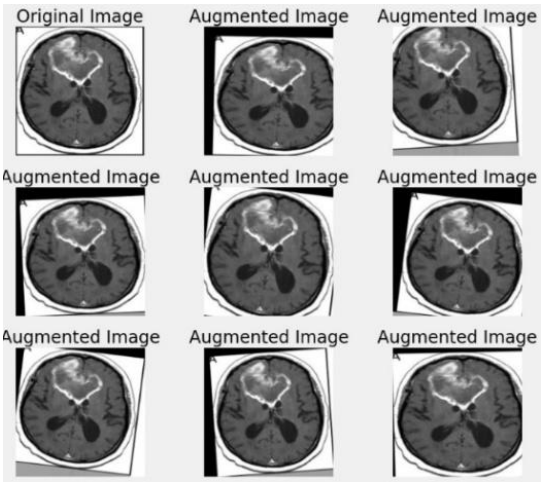

Fig. 7. Augmented images after rotation

2.3. Multi-scale processing

Analysing the regions with the tumour at different scales may help the model capture features at various resolutions, which is very beneficial for the detection of tumours, particularly the detection of tumours of various sizes. This is useful for the detection and categorization of brain tumours, which differ

widely in size and appearance. The model can pick up fine and coarse details by considering the image at different scales, which, in general, provides a better insight into the characteristics of the tumour. The general idea behind multi-scale processing is to build several versions of the same image at different scales. Processed in parallel, extracted features of the other scales are combined in a common representation. Multi-scale processing can be represented as:

$$I(\text{multi\_scale}) = Is(x, y)|s \in S \quad (13)$$

where Is(x,y) is the image at scale s and S is the set of scales.

2.4. Proposed multilayered max-norm regularization

Figure 8 shows the proposed architecture for the brain tumour classification. In this augmented and Multi-Layered regularized CNN architecture, the input layer consisted of channels corresponding to the T1, T2, and FLAIR modalities of the MRI images. These channels were fed into stacked convolutional layers with ReLU activation functions to extract high-level features from the input data. Also, Kernel regularization techniques are employed to get into more generalization. The L2 regularization (also known as weight decay) is used to prevent overfitting by penalizing large weights in deep learning models. The regularized loss function for a neural network layer with L2 regularization can be expressed as:

$$\text{Loss}_{\text{regularized}} = \text{Loss}_{\text{original}} + \frac{\lambda}{2}\sum_{i=1}^{n} w_i^2 \quad (14)$$

where λ – regularization parameter controlling the strength of regularization, n – number of weights in the layer, w_i – individual weights of the layer.

The term $\frac{\lambda}{2}\sum_{i=1}^{n} w_i^2$ adds a penalty to the loss function based on the squared magnitudes of the weights w_i. This encourages smaller weights, which can lead to a simpler model that is less prone to overfitting.

In standard L2 regularization, the loss function is modified as:

$$\text{Loss}_{\text{regularized}} = \text{Loss}_{\text{original}} + \frac{\lambda}{2}\sum_{l} |W^{(l)}|_F^2 \quad (15)$$

For layer-wise L2 regularization, where each layer (l) has a different regularization parameter (λ_l), the loss function becomes:

$$\text{Loss}_{\text{regularized}} = \text{Loss}_{\text{original}} + \sum_{l} \frac{\lambda_l}{2} |W^{(l)}|_F^2 \quad (16)$$

Here, ($W^{(l)}$) represents the weights of the layer (l), and ($|\cdot|_F$) denotes the Frobenius norm.

The proposed multilayered max-norm regularization is a technique that combines max-norm constraints with layer-specific regularization parameters to control the magnitude of weights across different layers of a neural network.

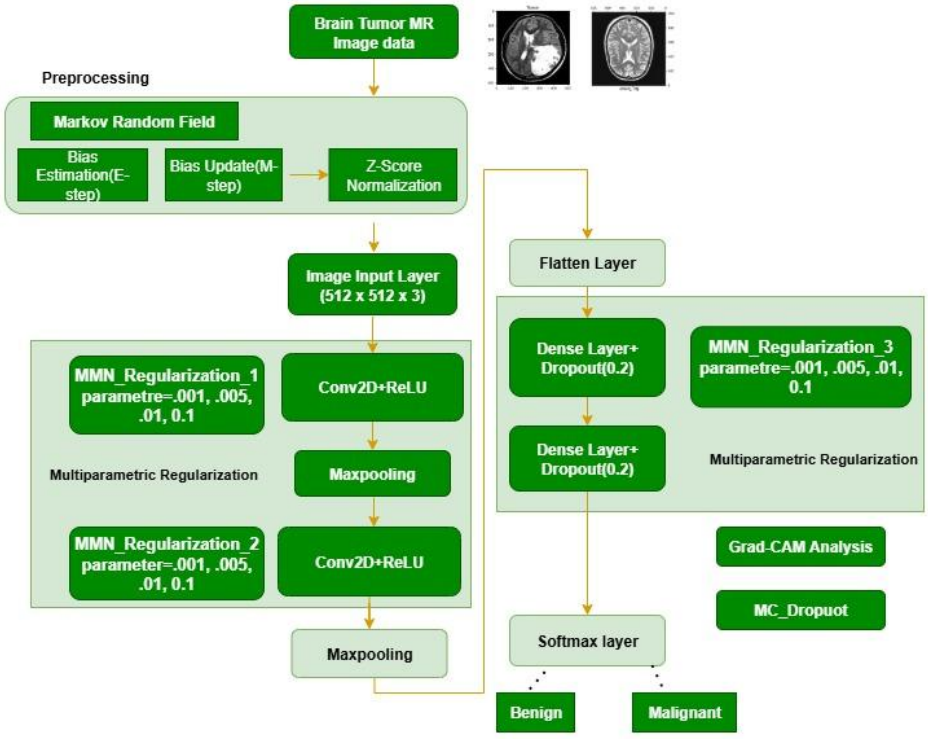

Fig. 8. Block diagram of the proposed model with Markov random field and max-norm regularization model

2.5. Max-norm constraint

The max-norm constraint is applied to the weights of each neuron w in a layer, ensuring that the Euclidean norm $|w|$ does not exceed a predefined maximum value r: $|w| \leq r$

This constraint is enforced during the training of the neural network to prevent the weights from growing too large, which can lead to instability and overfitting.

2.6. Effect on regularization parameter

The gradient of the regularized loss function with respect to the weights wi is modified as follows:

$$\frac{\partial \text{Loss}_{\text{regularized}}}{\partial w_i} = \frac{\partial \text{Loss}_{\text{original}}}{\partial w_i} + \lambda w_i \quad (17)$$

Equation (17) shows that L2 regularization adds a gradient term λw_i to the original gradient $\frac{\partial \text{Loss}_{\text{original}}}{\partial w_i}$. This modified gradient nudges the weights w_i towards smaller values during the training process. Higher values of λ impose stronger penalties on large weights, while smaller values allow more freedom for weights to grow. The following is the training and validation procedure used in this work. Also, the pseudo-code is shown in the following paragraph.

1. Splitting the Data: Divide the dataset into training, validation, and test sets.
2. Training with Different λ: Train the model using different λ values on the training set.
3. Evaluation on Validation Set: Evaluate model performance (e.g., accuracy, loss) on the validation set for each λ.
4. Selecting the Best λ: Choose the λ that gives the best performance on the validation set.
5. Final Evaluation: Assess the final model performance using the selected λ on the test set to estimate generalization ability.

Algorithm 1:

Training and Evaluation with Different Regularization Parameters

1: Input: Training data D_train, validation data D_val, regularization parameters Λ = {λ1, λ2, λ3, λ4, λ5, λ6}

2: Output: Best regularization parameter λ∗

3: Split D_train into D_train and D_val

4: for each λ ∈ Λ do

5: Train model on Dtrain train with regularization parameter λ

6: Evaluate model on Dval to get validation metrics (e.g., accuracy, loss)

7: Store validation metrics and λ

8: end for

9: Select λ ∗ with the best validation metrics

10: Train the final model on D_train with λ∗

11: Evaluate the final model on test data D_test to estimate the generalization ability

12: return λ∗

The model is trained on different λ values, and the results are shown in Table 2. Batch normalization layers were incorporated to stabilize and accelerate the training process by normalizing each layer's activations and enhancing the model's ability to identify subtle differences between tumour-present and tumour-absent images. A feature fusion layer was included to integrate information from different modalities, leveraging the complementary nature of the modalities for better classification performance. Finally, fully connected layers were used to combine the extracted features and perform the final classification, followed by a softmax output layer to output the probability of each class (tumour-present or tumour-absent). Overall, this architecture was designed to effectively handle the complexities of multimodal MRI data and achieve high accuracy in brain tumour classification.

Table 2. Comparison of model performance with different λ

λ	Learning Rate	Batch Size	Epochs	Testing Accuracy (%)	Computation Time (ms/step)
0.001	0.01	32	50	99.44	120
0.005	0.01	32	50	98.90	118
0.01	0.01	32	50	98.80	115
0.05	0.01	32	50	97.50	113
0.1	0.01	32	50	97.00	110
1.0	0.01	32	50	95.50	105

2.7. Uncertainty quantification using Monte Carlo dropout

To enable uncertainty quantification in our classification model, we adopted Monte Carlo (MC) dropout, a practical approximation to Bayesian inference in deep neural networks. During both training and inference, dropout layers are retained and activated to introduce stochasticity into the model. By performing multiple forward passes – each with a different subset of neurons dropped out – we obtain a distribution of predictions for the same input. Specifically, for each test sample, we conducted N = 50 stochastic forward passes, capturing the model's output distribution. The predictive mean represents the final class probability, while the standard deviation quantifies epistemic uncertainty, reflecting the model's confidence in its prediction. This methodology is particularly effective for medical imaging tasks, as it allows the detection of ambiguous or borderline cases where the model may be less certain. By identifying high-uncertainty predictions, the framework supports risk-aware decision-making, offering valuable insight for clinical validation and interpretability.

2.8. Explainable AI using Grad-CAM

We used Explainable Artificial Intelligence (XAI) techniques, notably Grad-CAM, to visualise and understand the decisions made by our CNN model in order to improve the interpretability of the model's prediction outputs. Grad-CAM generates a coarse localisation map that highlights significant areas in the input picture for class prediction by utilising the gradients of a target class that flow into the CNN's last convolutional layer. Grad-CAM creates a heatmap that shows the spatial regions in the input that made the biggest contribution to the prediction by calculating the gradient of the projected class score in relation to the feature maps of the final convolutional layer. To highlight tumour regions or other crucial areas that affected the model's prediction, we ran each test image through the trained CNN model, extracted the gradient information at the final convolutional layer, and then calculated the corresponding Grad-CAM heatmaps and superimposed them on the original MRI images. The combination of Grad-CAM with Monte Carlo Dropout-based uncertainty estimation forms a robust XAI framework, allowing both spatial insight (via heatmaps) and statistical confidence (via uncertainty quantification), thereby improving trust and transparency in automated medical diagnosis.

To evaluate the performance of the proposed model, we use key metrics such as Accuracy (%), Specificity (%), F1-Score (%), Precision (%), and Recall (%) as shown in the (18)–(22).

$$\text{Precision}(\%) = \frac{T\_P \times 100}{T\_P + F\_P} \tag{18}$$

$$\text{Recall}(\%) = \frac{T\_P \times 100}{T\_P + F\_N} \tag{19}$$

$$\text{F1\_Score}(\%) = 2 \times \frac{\text{Pres} \times \text{Rec}}{\text{Pres} + \text{Rec}} \tag{20}$$

$$\text{Accuracy}(\%) = \frac{T\_P + T\_N \times 100}{T\_P + T\_N + F\_P + F\_N} \tag{21}$$

$$\text{Specificity}(\%) = \frac{T\_N \times 100}{T\_N + F\_P} \tag{22}$$

3. Results

The analysis of the Multilayered Max-Norm Regularization (MMNR-CNN) model using multiple regularization techniques with augmentation in MRI multimodal images for the classification of brain tumours demonstrated significant improvements in performance metrics. By integrating data augmentation techniques such as Z-score Normalization, rotations, translations, and scaling, the model's robustness was enhanced, allowing it to generalize better to new data. The use of L2 regularization, with varying values of the regularization parameter (λ), helped in mitigating overfitting and improving the generalization capabilities of the model. Our experiments showed that a (λ) value of 0.001 provided the best balance between bias and variance, achieving a validation accuracy of 99.88%, precision of 100%, recall of 99.78%, specificity of 100%, and an F1 score of 99.88%. These results indicate a marked improvement over previous methodologies, showcasing the efficacy of our approach in accurately classifying brain tumours in multimodal MRI images.

The fine-tuning process with Multilayered Max-Norm Regularization (MMNR), coupled with the incorporation of dropout and batch normalization, further stabilized the training, leading to consistent and reliable model performance across various evaluation metrics. This comprehensive approach underscores the potential of advanced regularization and augmentation techniques in enhancing the diagnostic accuracy of deep learning models for medical image analysis. Fig. 9, 10, and 11 show the training and validation accuracy for the last 3(λ) values. The corresponding confusion matrix is shown in Fig. 12–14.

The ROC curve is a graphical representation of the model's diagnostic ability. The AUC value is 1 for both classes in the proposed model. A higher AUC value indicates better model performance. The ROC curve for this study is shown in Figure 15.

The model's predictions were visualized to further assess its performance. Figure 16 shows examples of prediction images, showing the model's ability to accurately classify brain tumours.

In addition to these metrics, the study included visual aids such as accuracy and loss plots throughout the training epochs. These plots provided insights into the model's learning dynamics, showcasing steady convergence and stability in performance. Moreover, the confusion matrix offered a detailed breakdown of the model's predictive performance across different tumour types, highlighting areas of strength (high true positives and true negatives) and areas for potential improvement (minimizing false positives and false negatives). This comprehensive analysis not only underscores the effectiveness of integrating multiple regularization techniques and augmentation strategies but also provides a clear understanding of how these methodologies contribute to the overall diagnostic accuracy of deep learning models in medical image analysis.

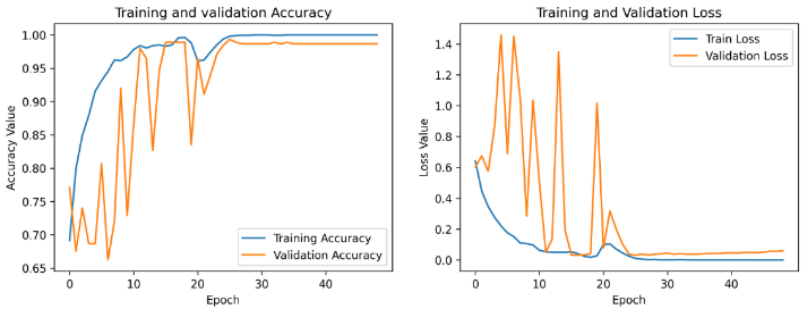

Fig. 9. Training and validation accuracy with λ = 0.01

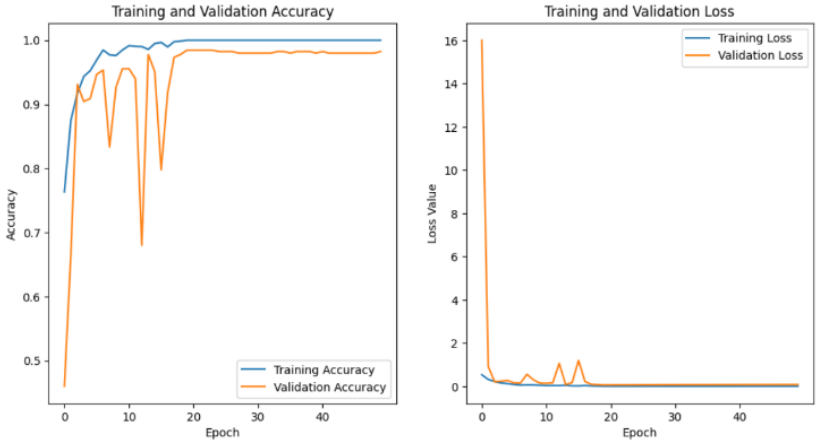

Fig. 10. Training and validation accuracy with λ = 0.005

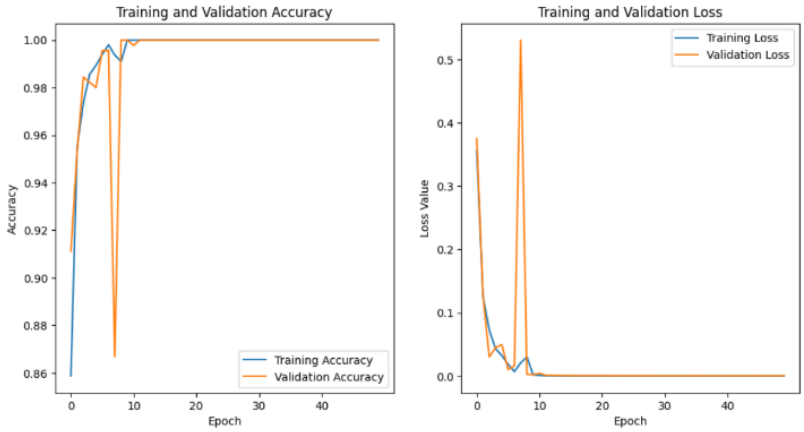

Fig. 11. Training and validation accuracy with λ = 0.001

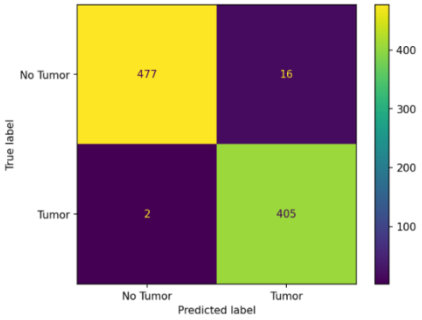

Fig. 12. Confusion matrix with λ = 0.01

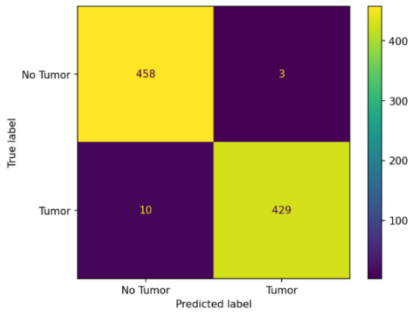

Fig. 13. Confusion matrix with λ = 0.005

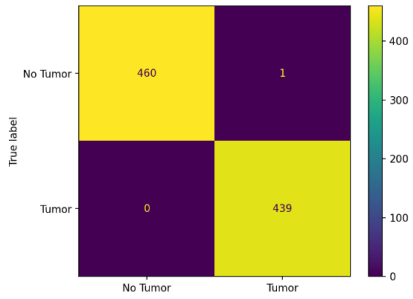

Fig. 14. Confusion matrix with λ = 0.001

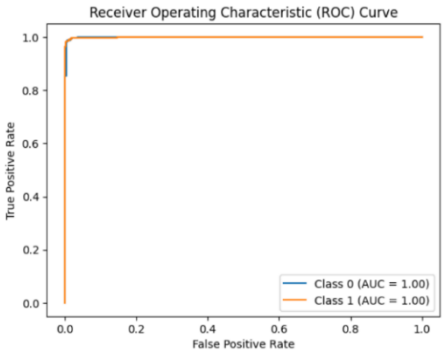

Fig. 15. ROC curve with λ = 0.001

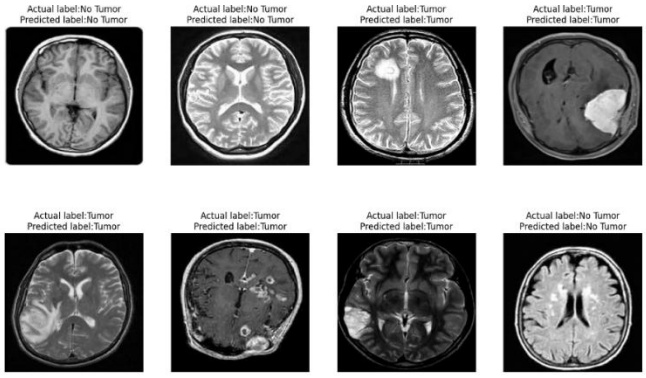

Fig. 16. Model prediction for different tumour types

3.1. Monte Carlo dropout & uncertainty estimation

To assess model robustness and predictive reliability, Monte Carlo Dropout was employed during inference to introduce stochasticity and estimate uncertainty in predictions. As summarized in Table 3, the majority of correctly predicted samples showed high confidence (mean probability > 0.98) and low uncertainty (standard deviation < 0.02), indicating the model's certainty in its decisions. Misclassified instances, in contrast, often had noticeably higher uncertainty values (e.g., 0.27 or 0.30), demonstrating the effectiveness of uncertainty estimation in identifying ambiguous or error-prone predictions. This aligns with the expected behaviour of MC Dropout in deep learning, where predictive variance serves as a proxy for epistemic uncertainty, guiding both human verification and further active learning strategies.

Table 3. Monte Carlo dropout-based prediction results on BR35H test set

Image #	True Label	Predicted Label	Confidence (Mean)	Uncertainty (Std Dev)
1	NO	NO	0.7394	0.3076
2	NO	NO	0.9970	0.0052
3	NO	NO	0.9838	0.0206
4	NO	YES	0.9167	0.1385
5	NO	NO	1.0000	0.0000
6	YES	YES	0.9994	0.0013
7	YES	YES	0.9969	0.0052
8	YES	NO	0.7451	0.2719
9	YES	YES	0.9864	0.0163
10	YES	YES	0.9923	0.0090

We employed 50 stochastic forward passes on the test dataset to assess the reliability of the model's prediction. The standard deviation of the class probability distribution across these passes was used as a proxy for predictive uncertainty. A histogram of the maximum standard deviations across all test images is shown in Figure 17. The majority of samples showed low predictive uncertainty (standard deviation < 0.1), indicating high confidence in predictions. A smaller subset exhibited moderate to high uncertainty, typically corresponding to ambiguous or borderline cases such as low-contrast tumour regions or overlapping structural patterns. This uncertain information is valuable for flagging samples requiring further expert review or additional diagnostic imaging. This uncertainty-aware classification framework thus adds an interpretable layer of safety to the deep learning model.

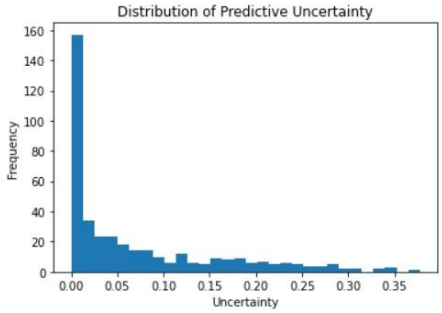

Fig. 17. Histogram showing the distribution of predictive uncertainty (maximum standard deviation) across 400 test MRI images

3.2. Explainable AI using Grad-CAM

To enhance the interpretability of the classification model, we employed Gradient-weighted Class Activation Mapping (Grad-CAM) to visualize class-specific discriminative regions in MRI images. Grad-CAM heatmaps were generated for 200 test images, as shown in Figure 18, overlaying the activation maps on the original MRI scans. These visualizations confirmed that the proposed model consistently focused on clinically relevant regions specifically the tumour cores and surrounding tissues for making predictions. For correctly classified cases, the heatmaps were well-aligned with the visible tumour masses, indicating that the model leveraged valid radiological features.

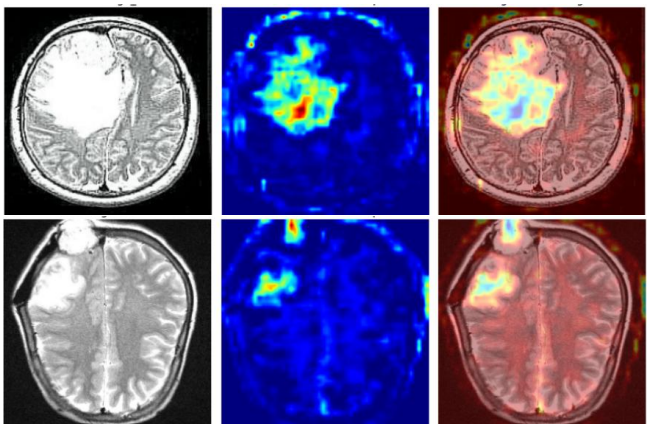

Fig. 18. Correctly classified: Visualization of Grad-CAM heatmaps overlaid on original MRI images. The highlighted regions correspond to the area's most influential in the model's decision-making process

In misclassified, as shown in Figure 19 or ambiguous instances, Grad-CAM revealed that the attention was either diffused across non-specific brain regions or cantered on areas outside the lesion, offering valuable cues about model uncertainty or dataset biases. These insights not only aid in validating the decision-making process of the model but also promote trust and transparency in AI-driven diagnostic systems. Furthermore, the use of Grad-CAM allows radiologists to verify AI predictions, making it a practical tool for clinical deployment in high-stakes environments like brain tumour diagnosis.

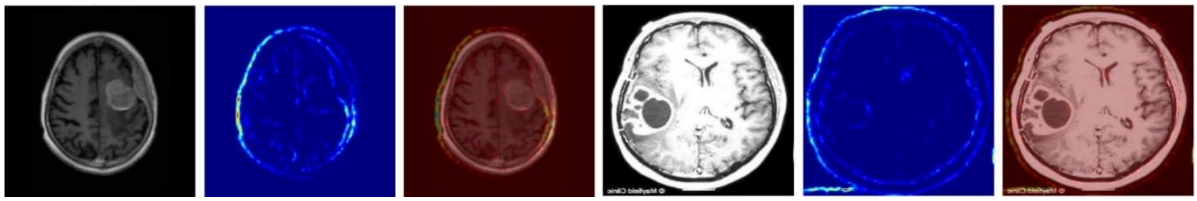

Fig. 19. Grad-CAM heatmaps overlaid on misclassified MRI images. The tumour regions are not separable in the blue colour image, which is most influential in the model's incorrect predictions

Table 4. Comparison of proposed method with recent publication on brain tumour classification using Br35H kaggle data

Publication	Methodology	Accuracy (%)	Precision (%)	Recall (%)	Specificity (%)	F1 Score (%)
Amran et al. (2022) [4]	Hybrid deep network	99.20	99.10	98.60	98.20	98
Gómez-Guzmán et al. (2023) [12]	CNN on MRIs	97.12	97.97	93.7	-	-
Ata et al. (2023) [5]	Improved deep structure	98.22	-	-	-	-
Bourennane et al. (2024) [6]	Cubic-SVM	99.7	99.7	99.7	-	99.7
Shah et al. (2023) [24]	Deep learning models	97.86	-	-	-	-
Eker et al. (2023) [9]	CoAtNet	98.26	-	-	-	-
Proposed Model	MMNR-with MRF	99.88	100	99.78	100	99.88

Table 4 shows the comparison of the proposed model with the recent publications available in the literature. It highlights the performance metrics of our model against those of recent advancements in the field of medical imaging [18, 19] and brain tumour analysis. This comparison underscores the improvements achieved by our approach.

4. Discussions

The results of this study demonstrate the effectiveness of the proposed Multilayered Max-Norm Regularization Convolutional Neural Network (MMNR-CNN) for brain tumour classification using multi-modal MRI images. The comparative analysis across varying values of the regularization parameter λ clearly showed that a balanced setting ($\lambda = 0.001$) provides the best trade-off between under fitting and overfitting, yielding superior accuracy, precision, recall, and F1 score. One of the important strengths of this work is the use of Monte Carlo Dropout, which helped us assess the confidence and uncertainty in the model's predictions. In real clinical settings, it is crucial not only to give predictions but also to indicate how certain the model is. Our results showed that when the model made correct predictions, it was usually very confident, while in the misclassified cases, the uncertainty was visibly higher. The Grad-CAM visually shows which part of the MRI scan influenced the model's decision. In most of the correctly classified images, the model focused on the tumour regions, which indicates that it is learning the right features. However, in the few wrongly classified cases, the attention was either scattered or misplaced, pointing towards possible limitations in the dataset or model understanding. The MMNR-CNN model not only achieves high accuracy but also builds trust through explainability and uncertainty analysis. Such features are essential if we are to see AI tools used confidently by medical professionals in real-world clinical practice.

5. Conclusion

In the current work, we introduced MMNR-CNN, which is a deep learning model to perform the classification of brain tumours based on multi-modal MRI images. Some regularization methods, such as max-norm, L2 regularization, dropout and batch normalization methods, were well applied in the design of the model to enhance prediction accuracy and reliability.

We also used Monte Carlo Dropout in inference to estimate the uncertainty of the model. Besides the ability to make accurate predictions, this allowed us to measure the level of confidence that our model has in its ruling, which is absolutely essential in medical applications of AI. Our results indicated the usefulness of the model in aiding medical practitioners because it showed a significant amount of confidence in making correct predictions with a greater amount of uncertainty among those questioned or mistakenly coded.

Moreover, we generated heatmaps, which graphically explain how the model makes decisions based on Grad-CAM. In most of instances, such visualizations helped in establishing that indeed the model was focusing on the right tumour areas. Grad-CAM assisted us in identifying potential causes of model errors, such as overlapping image features with high grade tumour or poor image quality.

The suggested MMNR-CNN model demonstrated not only great accuracy but also robustness and explainability. It can be used to a significant extent by diagnostic facilities and hospitals operating in the framework of which doctors will benefit due to the accessible and trusted services of an AI. The model has a high chance of being utilized practically in the field of brain tumour diagnosis due to the effectiveness of brain tumour classification, the ability to provide uncertainty estimation, and visual interpretation.

Acknowledgment

The authors express sincere gratitude to APJ Abdul Kalam Technological University, Thiruvananthapuram, Kerala, for their invaluable assistance in making this initiative feasible through academic support.

References

[1] Akbari, H., Macyszyn, L., Da, X., Wolf, R. L., Bilello, M., Verma, R., O'Rourke, D. M., & Davatzikos, C. (2014). Pattern Analysis of Dynamic Susceptibility Contrast-enhanced MR Imaging Demonstrates Peritumoral Tissue Heterogeneity. *Radiology*, *273*(2), 502–510. https://doi.org/10.1148/radiol.14132458

[2] Akkus, Z., Galimzianova, A., Hoogi, A., Rubin, D. L., & Erickson, B. J. (2017). Deep Learning for Brain MRI Segmentation: State of the Art and Future Directions. *Journal of Digital Imaging*, *30*(4), 449–459. https://doi.org/10.1007/s10278-017-9983-4

[3] Ammar, L. B., Gasmi, K., & Ltaifa, I. B. (2024). ViT-TB: Ensemble Learning Based ViT Model for Tuberculosis Recognition. *Cybernetics and Systems*, *55*(3), 634–653. https://doi.org/10.1080/01969722.2022.2162736

[4] Amran, G. A., Alsharam, M. S., Blajam, A. O. A., Hasan, A. A., Alfaifi, M. Y., Amran, M. H., Gumaei, A., & Eldin, S. M. (2022). Brain Tumor Classification and Detection Using Hybrid Deep Tumor Network. *Electronics*, *11*(21), 3457. https://doi.org/10.3390/electronics11213457

[5] Ata, M. M., Yousef, R. N., Khalid Karim, F., & Sami Khafaga, D. (2023). An Improved Deep Structure for Accurately Brain Tumor Recognition. *Computer Systems Science and Engineering*, *46*(2), 1597–1616. https://doi.org/10.32604/csse.2023.034375

[6] Bourennane, M., Naimi, H., & Mohamed, E. (2024). Deep Feature Extraction with Cubic-SVM for Classification of Brain Tumor. *Studies in Engineering and Exact Sciences*, *5*(1), 19–35. https://doi.org/10.54021/seesv5n1-002
[7] Chang, K., Bai, H. X., Zhou, H., Su, C., Bi, W. L., Agbodza, E., Kavouridis, V. K., Senders, J. T., Boaro, A., Beers, A., Zhang, B., Capellini, A., Liao, W., Shen, Q., Li, X., Xiao, B., Cryan, J., Ramkissoon, S., Ramkissoon, L., … Kalpathy-Cramer, J. (2018). Residual Convolutional Neural Network for the Determination of *IDH* Status in Low- and High-Grade Gliomas from MR Imaging. *Clinical Cancer Research*, *24*(5), 1073–1081. https://doi.org/10.1158/1078-0432.CCR-17-2236
[8] Das, S., & Goswami, R. S. (2023). Review, Limitations, and future prospects of neural network approaches for brain tumor classification. *Multimedia Tools and Applications*, *83*(15), 45799–45841. https://doi.org/10.1007/s11042-023-17215-7
[9] Eker, A. G., Korkmaz Erdem, G., & Duru, N. (2023). Categorical and Binary Brain Tumor Classification Using Transfer Learning Techniques. *Sivas Cumhuriyet Üniversitesi Mühendislik Fakültesi Dergisi*, *1*(1), 11–16.
[10] Feng, Y., Gao, J., Yang, S., & Xu, C. (2023). Spatial-Temporal Exclusive Capsule Network for Open Set Action Recognition. *IEEE Transactions on Multimedia*, *25*, 9464–9478. https://doi.org/10.1109/TMM.2023.3252275
[11] Ghafoorian, M., Mehrtash, A., Kapur, T., Karssemeijer, N., Marchiori, E., Pesteie, M., Guttmann, C. R. G., De Leeuw, F.-E., Tempany, C. M., Van Ginneken, B., Fedorov, A., Abolmaesumi, P., Platel, B., & Wells, W. M. (2017). Transfer Learning for Domain Adaptation in MRI: Application in Brain Lesion Segmentation. In M. Descoteaux, L. Maier-Hein, A. Franz, P. Jannin, D. L. Collins, & S. Duchesne (Eds), *Medical Image Computing and Computer Assisted Intervention − MICCAI 2017* (Vol. 10435, pp. 516–524). Springer International Publishing. https://doi.org/10.1007/978-3-319-66179-7_59
[12] Gómez-Guzmán, M. A., Jiménez-Beristaín, L., García-Guerrero, E. E., López-Bonilla, O. R., Tamayo-Perez, U. J., Esqueda-Elizondo, J. J., Palomino-Vizcaino, K., & Inzunza-González, E. (2023). Classifying Brain Tumors on Magnetic Resonance Imaging by Using Convolutional Neural Networks. *Electronics*, *12*(4), 955. https://doi.org/10.3390/electronics12040955
[13] Havaei, M., Davy, A., Warde-Farley, D., Biard, A., Courville, A., Bengio, Y., Pal, C., Jodoin, P.-M., & Larochelle, H. (2017). Brain tumor segmentation with Deep Neural Networks. *Medical Image Analysis*, *35*, 18–31. https://doi.org/10.1016/j.media.2016.05.004
[14] Havaei, M., Guizard, N., Chapados, N., & Bengio, Y. (2016). HeMIS: Hetero-Modal Image Segmentation. In S. Ourselin, L. Joskowicz, M. R. Sabuncu, G. Unal, & W. Wells (Eds), *Medical Image Computing and Computer-Assisted Intervention – MICCAI 2016* (Vol. 9901, pp. 469–477). Springer International Publishing. https://doi.org/10.1007/978-3-319-46723-8_54
[15] Kamnitsas, K., Ledig, C., Newcombe, V. F. J., Simpson, J. P., Kane, A. D., Menon, D. K., Rueckert, D., & Glocker, B. (2017). Efficient multi-scale 3D CNN with fully connected CRF for accurate brain lesion segmentation. *Medical Image Analysis*, *36*, 61–78. https://doi.org/10.1016/j.media.2016.10.004
[16] Li, Y., Wang, J., Hu, M., Patel, P., Mao, H., Liu, T., & Yang, X. (2023). Prostate gleason score prediction via MRI using capsule network. In K. M. Iftekharuddin & W. Chen (Eds), *Medical Imaging 2023: Computer-Aided Diagnosis* (p. 72). SPIE. https://doi.org/10.1117/12.2653621
[17] Litjens, G., Kooi, T., Bejnordi, B. E., Setio, A. A. A., Ciompi, F., Ghafoorian, M., Van Der Laak, J. A. W. M., Van Ginneken, B., & Sánchez, C. I. (2017). A survey on deep learning in medical image analysis. *Medical Image Analysis*, *42*, 60–88. https://doi.org/10.1016/j.media.2017.07.005
[18] Liu, Z., Tong, L., Chen, L., Jiang, Z., Zhou, F., Zhang, Q., Zhang, X., Jin, Y., & Zhou, H. (2023). Deep learning based brain tumor segmentation: A survey. *Complex & Intelligent Systems*, *9*(1), 1001–1026. https://doi.org/10.1007/s40747-022-00815-5
[19] Louis, D. N., Perry, A., Reifenberger, G., Von Deimling, A., Figarella-Branger, D., Cavenee, W. K., Ohgaki, H., Wiestler, O. D., Kleihues, P., & Ellison, D. W. (2016). The 2016 World Health Organization Classification of Tumors of the Central Nervous System: A summary. *Acta Neuropathologica*, *131*(6), 803–820. https://doi.org/10.1007/s00401-016-1545-1
[20] M.C, B., R.S, S. R., & Thomas, V. (2026). CBAM–SMK: Integrating Convolution Block Attention Module with separable multi-resolution kernels in deep neural networks for brain tumor classification. *Biomedical Signal Processing and Control*, *112*, 108483. https://doi.org/10.1016/j.bspc.2025.108483
[21] Menze, B. H., Jakab, A., Bauer, S., Kalpathy-Cramer, J., Farahani, K., Kirby, J., Burren, Y., Porz, N., Slotboom, J., Wiest, R., Lanczi, L., Gerstner, E., Weber, M.-A., Arbel, T., Avants, B. B., Ayache, N., Buendia, P., Collins, D. L., Cordier, N., … Van Leemput, K. (2015). The Multimodal Brain Tumor Image Segmentation Benchmark (BRATS). *IEEE Transactions on Medical Imaging*, *34*(10), 1993–2024. https://doi.org/10.1109/TMI.2014.2377694
[22] Saurav, S., Sharma, A., Saini, R., & Singh, S. (2023). An attention-guided convolutional neural network for automated classification of brain tumor from MRI. *Neural Computing and Applications*, *35*(3), 2541–2560. https://doi.org/10.1007/s00521-022-07742-z
[23] Shah, H. A., Saeed, F., Yun, S., Park, J.-H., Paul, A., & Kang, J.-M. (2022). A Robust Approach for Brain Tumor Detection in Magnetic Resonance Images Using Finetuned EfficientNet. *IEEE Access*, *10*, 65426–65438. https://doi.org/10.1109/ACCESS.2022.3184113
[24] Shah, K., Shah, K., Chaudhari, A., & Kothadiya, D. (2024). Comprehensive Analysis of Deep Learning Models for Brain Tumor Detection from Medical Imaging. In S. J. Nanda, R. P. Yadav, A. H. Gandomi, & M. Saraswat (Eds), *Data Science and Applications* (Vol. 819, pp. 339–351). Springer Nature Singapore. https://doi.org/10.1007/978-981-99-7820-5_28
[25] Sharif, M. I., Li, J. P., Khan, M. A., & Saleem, M. A. (2020). Active deep neural network features selection for segmentation and recognition of brain tumors using MRI images. *Pattern Recognition Letters*, *129*, 181–189. https://doi.org/10.1016/j.patrec.2019.11.019
[26] Sharma, A. K., Nandal, A., Dhaka, A., Zhou, L., Alhudhaif, A., Alenezi, F., & Polat, K. (2023). Brain tumor classification using the modified ResNet50 model based on transfer learning. *Biomedical Signal Processing and Control*, *86*, 105299. https://doi.org/10.1016/j.bspc.2023.105299
[27] Shin, H.-C., Roth, H. R., Gao, M., Lu, L., Xu, Z., Nogues, I., Yao, J., Mollura, D., & Summers, R. M. (2016). Deep Convolutional Neural Networks for Computer-Aided Detection: CNN Architectures, Dataset Characteristics and Transfer Learning. *IEEE Transactions on Medical Imaging*, *35*(5), 1285–1298. https://doi.org/10.1109/TMI.2016.2528162
[28] Sun, G., Ding, S., Sun, T., & Zhang, C. (2021). SA-CapsGAN: Using Capsule Networks with embedded self-attention for Generative Adversarial Network. *Neurocomputing*, *423*, 399–406. https://doi.org/10.1016/j.neucom.2020.10.092
[29] Tan, M., & Le, Q. V. (2019). *EfficientNet: Rethinking Model Scaling for Convolutional Neural Networks*. https://doi.org/10.48550/ARXIV.1905.11946
[30] Tandel, G. S., Tiwari, A., & Kakde, O. G. (2021). Performance optimisation of deep learning models using majority voting algorithm for brain tumour classification. *Computers in Biology and Medicine*, *135*, 104564. https://doi.org/10.1016/j.compbiomed.2021.104564
[31] Zhang, F., Li, Z., Zhang, B., Du, H., Wang, B., & Zhang, X. (2019). Multi-modal deep learning model for auxiliary diagnosis of Alzheimer's disease. *Neurocomputing*, *361*, 185–195. https://doi.org/10.1016/j.neucom.2019.04.093
[32] Zhang, F., Pan, B., Shao, P., Liu, P., Shen, S., Yao, P., & Xu, R. X. (2022). A Single Model Deep Learning Approach for Alzheimer's Disease Diagnosis. *Neuroscience*, *491*, 200–214. https://doi.org/10.1016/j.neuroscience.2022.03.026
[33] Zhou, Z., Rahman Siddiquee, M. M., Tajbakhsh, N., & Liang, J. (2018). UNet++: A Nested U-Net Architecture for Medical Image Segmentation. In D. Stoyanov, Z. Taylor, G. Carneiro, T. Syeda-Mahmood, A. Martel, L. Maier-Hein, J. M. R. S. Tavares, A. Bradley, J. P. Papa, V. Belagiannis, J. C. Nascimento, Z. Lu, S. Conjeti, M. Moradi, H. Greenspan, & A. Madabhushi (Eds), *Deep Learning in Medical Image Analysis and Multimodal Learning for Clinical Decision Support* (Vol. 11045, pp. 3–11). Springer International Publishing. https://doi.org/10.1007/978-3-030-00889-5_1

M.Tech. Mulackal Chandran Binish
e-mail: binishmc@mec.ac.in

M. C. Binish completed his B.Tech degree in Electronics and Communication Engineering from College of Engineering, Poonjar, India. He subsequently earned both his M.Tech degree in electronics (signal processing) from Cochin University of Science and Technology, India. Now, he is a research scholar at Model Engineering College under APJ Abdul Kalam Technological University.
His research interests include biomedical imaging, signal processing, and Artificial intelligence. He has worked on several research works on brain tumour classification and segmentation on advanced deep learning architectures, cognitive radio resource allocation etc.

https://orcid.org/0000-0002-2326-7723

Ph.D. Vinu Thomas
e-mail: vt@mec.ac.in

Vinu Thomas completed his B.Tech degree in electronics and communication engineering from the Mar Athanasius College of Engineering, Kothamangalam, India. He subsequently earned both his M.Tech degree in Electronics and Ph.D. degree from Cochin University of Science and Technology, India. He held the position of Principal at the Government. Model Engineering College from 2018 to 2021, and at the College of Engineering Cherthala from 2021 to 2022. Since 2022, he has been serving as the Dean (Academic) at APJ Abdul Kalam Technological University, the State University in Kerala, India. Dr. Thomas was awarded the prestigious Dr. K.G. Nair Endowment Award for achieving the top rank in the M.Tech program at Cochin University of Science and Technology in 2001. He is a member of the IEEE.
His research interests are focused on medical image processing, machine learning, deep learning, and computational electrodynamics.

https://orcid.org/0000-0003-1978-0273